Optimal Control Tuning of VSC-MTDC Using a Multi-objective Hybrid PSO Algorithm

Lawrence Bibaya
School of Electrical and Electronic Engineering
North China Electric Power University
Beijing, China
lawrencebibaya@ncepu.edu.cn

Chongru Liu
School of Electrical and Electronic Engineering
North China Electric Power University
Beijing, China
chongru.liu@ncepu.edu.cn

Gengyin Li
School of Electrical and Electronic Engineering
North China Electric Power University
Beijing, China
ligy@ncepu.edu.cn

Abstract— **In this paper, a hybrid particle swarm optimization (HPSO) algorithm to optimize the parameters of DC voltage margin controllers in a voltage source converters multi-terminal direct current (VSC-MTDC) system is proposed. The proposed approach presents a multi-objective function with different time intervals using integral of time-weighted absolute value of the error (ITAE), such that the voltage margin controllers will provide a minimum undershoot, minimum overshoot and fast settling time performance. The performance of the proposed approach is tested on a three-terminal VSC-MTDC system in PSCAD environment through time domain simulations, and comparison to controllers optimized by SIMPLEX algorithm confirmed the favorable performance of the proposed HPSO-tuned controllers.**

Keywords— VSC-MTDC, DC voltage margin, HPSO algorithm, optimization, ITAE.

I. INTRODUCTION

With the growing demand of energy and global environmental changes, more and more countries are concentrating towards clean and renewable energy. However, several sites for exploitation of renewable resources are usually remotely located from demand centers. Facing this situation, scholar's community is putting a considerable effort and it is witnessing the development of direct current technology systems over the last recent years. Dc technology owns many advantages related to the issue of how to efficiently transmit electrical energy over long distances [1-4]. Researchers from universities and power industry all over the world are holding the viewpoint that the novel MTDC technology based on voltage source converter (VSC), possesses great advantages in reliability improvement, in energy trading between regions, in maintenance and in independent control of active and reactive power [5-8]. The Nan'ao HVDC project involving China Southern Grid, which was initially a three-terminal system and commissioned in late 2013, is the first MTDC system based upon VSC technology[9].

Inside a VSC-MTDC network, direct voltage control is certainly one of the most important tasks given to VSC-HVDC stations. A well-controlled direct voltage on a HVDC grid requires a balanced power flow between all the interconnected stations[5]. Numerous papers investigated the coordinate control method of dc voltage, however, dc voltage control based voltage margin method and voltage droop methods are the ones mostly employed in literatures [6],[10-15].

The proper tuning of PI controller's parameters substantially influences the performance of the MTDC grid's control. Proportional gains adjustments vary the bandwidth to meet the settling time specification, and integral time constant are normally used to reduce steady state error [16]. The most HVDC systems practices often select PI parameters based on operator's experience[13],[17]. Recently, intelligent optimization algorithm like simplex algorithm[18],[19], genetic algorithm[20], and PSO algorithm [21-23] have been used to address this issue in MTDC system, but most of them focused on single converter stations optimization. However, some deficiencies appeared with the optimization of only one-station converters. In [24], a traditional PSO algorithm has been used on a back to back VSC-HVDC system, the approach used large numbers of iterations and particles in order to find optimal solutions which is really time consuming.

Despite good results of such papers, there are still some shortcomings in simultaneously addressing the issues of global optimal parameters, such as fast convergence approach and coordinated dc voltage control at VSC-MTDC level. In this paper a hybrid particle swarm optimization algorithm is adopted to optimize the PI parameters of voltage margin controllers in a VSC-MTDC system. Also a multi-objective function with different time intervals using ITAE is defined such that the voltage margin controllers will provide a minimum undershoot, minimum overshoot and fast settling time performance. The performance of the proposed approach is tested and examined on a three terminal VSC-MTDC system in PSCAD environment through time domain simulations under transient and steady state.

II. MODELING AND CONTROL OF VSC-MTDC GRIDS

VSC-MTDC grids are characterized by the interconnection of more than 2 VSC systems. The control of MTDC grids includes DC voltage regulation at DC terminals, control of active and reactive power at the point of common coupling (PCC), and maintaining the PCC's AC voltage.

The most commonly used control strategy for the VSC stations is based on the vector control [5],[12],[25]. So by employing modulation technique and vector control

978-1-5386-8549-5/18/$31.00

strategy, VSC stations can flexibly carry out decoupled control of active and reactive power as well as DC and AC voltage.

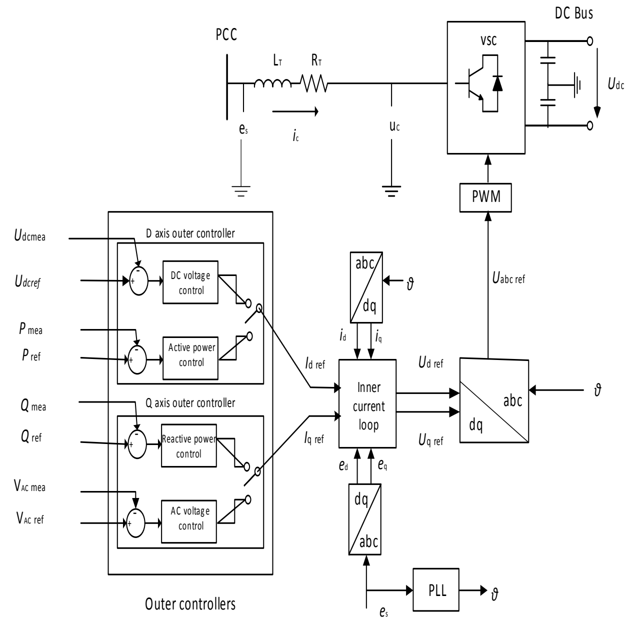

Fig.1. Architecture of vector control at a VSC station

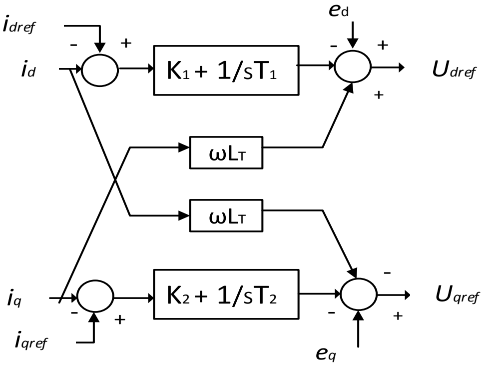

Fig.2. Structure of the Inner Current Controller

In vector control, the AC currents and voltages of the converter station (at the PCC) are transformed into the rotating direct-quadrature (d-q) reference frame, synchronized with the AC grid voltage by means of a phase-locked loop (PLL). Fig. 1 illustrates the general architecture of the vector control at a VSC-HVDC station.

A. Inner Current Controller

The inner current controller, includes fast proportional–integral (PI) controllers, which track the reference currents, set by the outer controllers, and produces the voltage reference for the converter (U_{dref} and U_{qref}). To derive the structure of the inner current controller, the voltage at PCC (e_s) and converter-side voltage (u_c) are related by,

$$e_s - u_c = R_T i_c + L_T \frac{di_c}{dt} \tag{1}$$

Where, i_c is the current flowing from PCC to the converter, and R_T and L_T represent the total resistance and inductance between the PCC and converter. Then by applying the Park transformation, (1) can be expressed in d-q reference frame by,

$$e_d - u_d = R_T i_d + L_T \frac{di_d}{dt} - \omega L_T i_q \tag{2}$$

$$e_q - u_q = R_T i_q + L_T \frac{di_q}{dt} - \omega L_T i_d \tag{3}$$

Where ω is the angular frequency of the AC voltage at the PCC. The structure of the inner current controller is obtained from (2)-(3) and is shown in Fig. 2. The reference voltages (U_{dref} and U_{qref}) are then transformed back into the *abc* reference frame and used to generate the switching signals for the converter.

B. Outer Controller

The outer controllers are responsible for generating the reference currents for the inner current controller (i_{dref} and i_{qref}) and they include the active and reactive channels, as shown in Fig. 1. The active channels are responsible for regulation of the active power or DC voltage while the reactive channels control the reactive power or amplitude of AC voltage at the PCC. For active power control, the power equations in d-q reference frame can be used,

$$P = u_d i_d \tag{4}$$

$$Q = -u_d i_q \tag{5}$$

To maintain the DC voltage at its reference value, the active power exchanged with the AC grid must be properly regulated. Hence, modification of the d-axis current (i_d) allows controlling the DC voltage within the permissible limits.

III. HYBRID PSO ALGORITHM AND OBJECTIVE FUNCTION

A. The ITAE Index

There are many minimum error indexes being used to measure the performance of control systems. ITAE (Integral of Time-weighted Absolute value of the Error) is one of these indexes. It can be expressed as (6)

$$J_{ITAE} = \int_0^T t.|e(t)|.dt \tag{6}$$

Where $|e(t)|$ is the function of the error of control variables (e.g. DC voltage, active power, reactive power) compared with the references and the upper limit T is a finite time chosen so that the integral approaches a steady-state value. Voltage margin block diagram is shown in Fig.3.

B. Objective Function

Compared to most of the papers that uses single objective function, this paper uses a multi-objective function divided into several time intervals where there is an active power step change for each time interval. Through this method, the system will be subjected to different operating conditions during the optimization process in order to find the optimal PI controller's parameters that will minimize the DC voltage, active and reactive powers errors. Because the VSC-MTDC possesses several control loops, the objective function will be to minimize the weighted sum of ITAE. The corresponding objective function can be expressed in (7) and (8),

$$O_f(X)=\sum_{i=1}^{n} m_i f_i(X) \tag{7}$$

$$\begin{aligned} f_i(X) &= \sum_{j=1}^{m} \omega_j ITAE_j \\ &= \sum_{j=1}^{m} \omega_j \int_0^T t.|e(t)|.dt \end{aligned} \tag{8}$$

Where f_i is the performance index for the i^{th} sub-objective, m_i is the weighting factor applied to the i^{th} sub-objective. ω_j is the weighting factor corresponding to the j^{th} controlled variables. m is the number controlled variables. n is the number of time intervals. Vector $X=(X_1,X_2,...X_n)$ is the control system parameters, i.e. PI parameters.

In this paper, all the weighting factors corresponding to the controlled variables (ω_j) are equal to one, except the one's corresponding to the DC voltage variable which is equal to two. The X in (7) and (8) will be a set of parameters of outer loops control, based on four active power steps changes within the simulation, and the fact that m_i=8 during the optimization process, the objective function for the MTDC system is given by:

$$\begin{aligned} O_f(X) &= \sum_{j=1}^{5} 8.f_i(X) \\ &= \sum_{j=1}^{8} \omega_j \int_0^{t_1} t.|e(t)|.dt + \sum_{j=1}^{8} \omega_j \int_{t_1}^{t_2} t.|e(t)|.dt + ... + \sum_{j=1}^{8} \omega_j \int_{t_4}^{t_5} t.|e(t)|.dt \end{aligned} \tag{9}$$

The lower and upper bounds of the PI parameters are defined as:

$$\left.\begin{aligned} &U_{dcref}, 0.01 \le K \le 20 \\ &U_{dcref}, 0.001 \le T \le 5 \\ &P_{1lref}, 0.01 \le K \le 20 \\ &P_{1lref}, 0.001 \le T \le 5 \\ &P_{1href}, 0.01 \le K \le 20 \\ &P_{1href}, 0.001 \le T \le 5 \\ &P_{2ref}, 0.01 \le K \le 20 \\ &P_{2ref}, 0.001 \le T \le 5 \\ &P_{3ref}, 0.01 \le K \le 20 \\ &P_{3ref}, 0.001 \le T \le 5 \\ &U_{dclref}, 0.01 \le K \le 20 \\ &U_{dclref}, 0.001 \le T \le 5 \\ &U_{dchref}, 0.01 \le K \le 20 \\ &U_{dchref}, 0.001 \le K \le 5 \\ &Q_{ref}, 0.01 \le K \le 20 \\ &Q_{ref}, 0.001 \le T \le 5 \end{aligned}\right\} \tag{10}$$

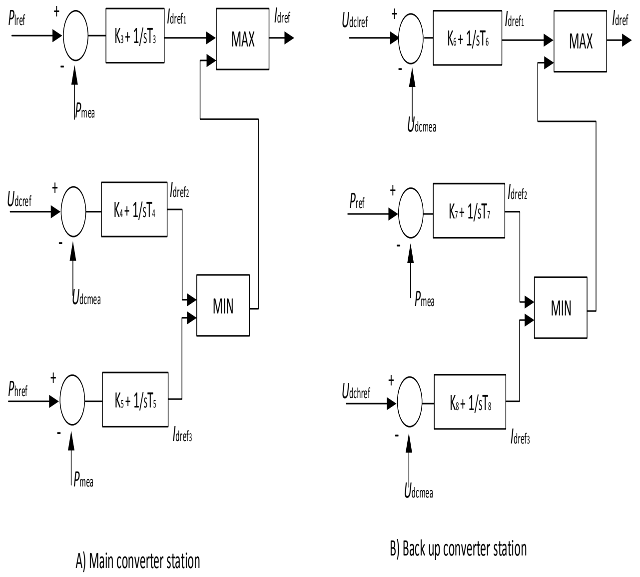

A) Main converter station

B) Back up converter station

Fig.3. Voltage Margin Method control block diagram

C. Hybrid PSO algorithm for optimization of DC Voltage Margin Controllers

PSO technique is an evolutionary computation technique based on the analogy of swarm of birds and fish schooling. At each iteration of the search process, particles dynamically adjust their positions and velocities by tracking their best position reached so far $P_{best.}$ and the best position reached so far in the group $G_{best.}$ The new position of the i^{th} particle is found by adding the velocity component as follows:

$$\begin{aligned} &v_j(i+1) = wv_j(i) + c_1 rand_1 \times (\mathrm{Pbest_j}(i) - \\ &X_j(i)) + c_2 rand_2 \times (\mathrm{Gbest}(i) - X_j(i)) \end{aligned} \tag{11}$$

$$X_j(i+1) = X_j(i) + v_j(i+1) \tag{12}$$

Where $v_j(i)$ is the velocity of the j^{th} particle at iteration i, w is the weighting function, c_1 and c_2 are the weighting coefficients, rand is a random number between 0 and 1, $X_j(i)$ is the current position of the j^{th} particle at iteration i.

- Adaptive weighting function

In traditional PSO algorithm, the value of w is fixed, which increases the possibility to be trapped in the local optimum. In the hybrid algorithm, an adaptive weighting function been adopted where large inertia weight is used to enhance global exploration at initial stages, and lower inertia weight is used for better local exploration at final stages. The adaptive weighting function will increase the possibility to reach the global optimum and is defined as:

$$w = w_{\max} - \frac{w_{\max} - w_{\min}}{iter_{\max}} \times iter \tag{13}$$

Where $w_{\max}$ is the initial weight, $w_{\min}$ is the final weight, $iter_{\max}$ is the maximum iteration number and $iter$ is the current iteration number.

- Elitism function

In classic PSO algorithm, the focus is on updating all the new particles positions based on their own experiences $P_{best.}$and the experiences of others $G_{best.}$ However, ensuring that the best solution known so far will remain in the population will definitely speed up the convergence of the research process. The preservation of the elite solution or elitism function will be implemented by always randomly replacing a particle in the current population by the $G_{best.}$

The hybrid PSO algorithm will quickly converges to the optimal PI parameters with just few initial parameters.

The flow chart of the process for parameters optimization is shown in Fig.4.

IV. SIMULATION STUDIES

A. *Three-terminal VSC-MTDC*

In order to verify the effectiveness of our optimal coordinated approach, a three–terminal VSC-MTDC system is built in PSCAD simulation software. And the structure of the system is shown in Fig.5. The test system is composed of three AC grids with terminal voltage of 10kV, the frequency is 50Hz, the transformer connection is 10kV/5kV, the rated voltage of the MTDC grid is 10kV, and the DC line resistance been neglected.

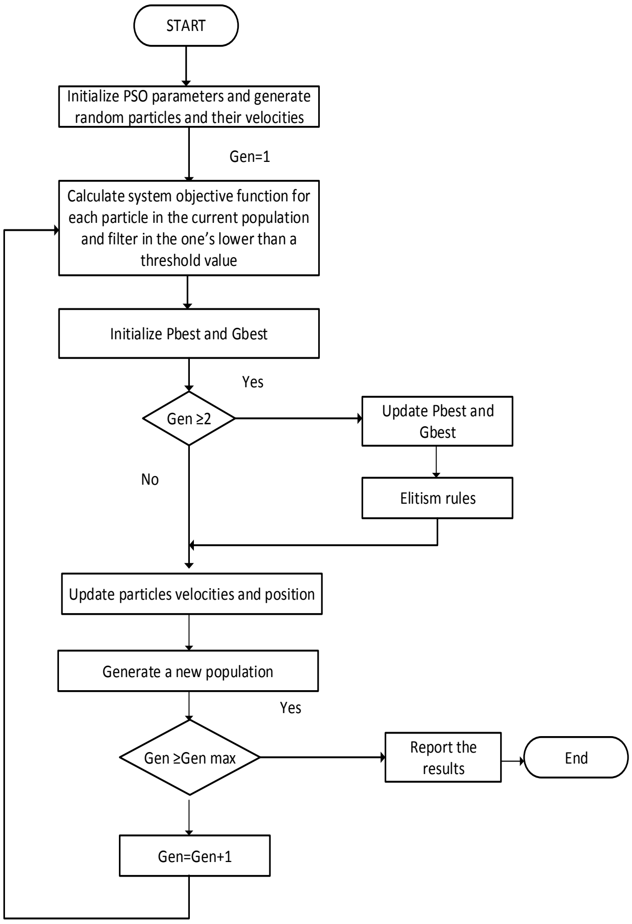

Fig.4. Flow chart of optimization process

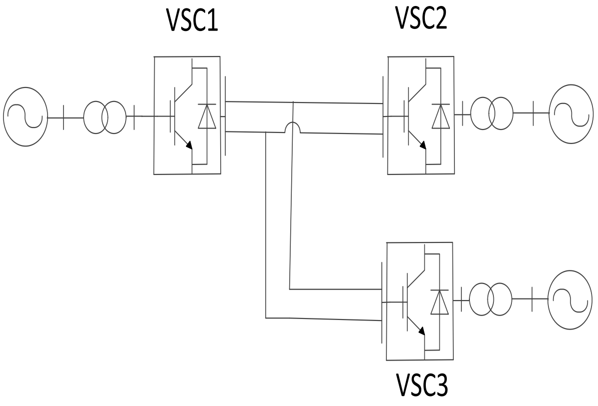

Fig.5. Structure of three-terminal VSC-MTDC

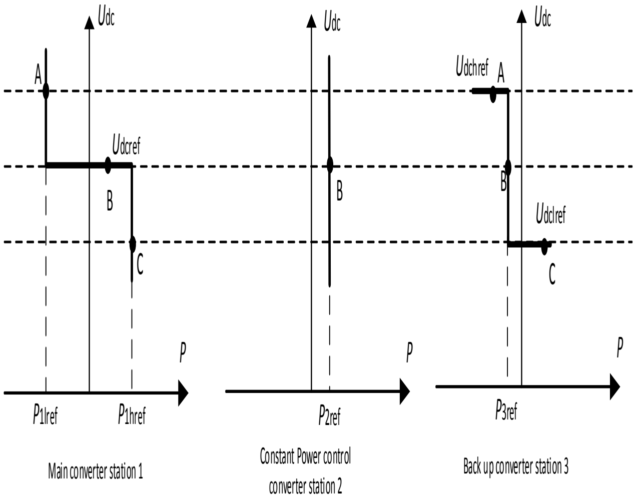

Fig.6. Three-terminal VSC-MTDC Voltage Margin Method P-U_{dc} characteristics curves

In Fig.6, VSC_1 and VSC_3 take DC voltage margin control as the outer loop control. VSC_2 takes constant active power control as the outer loop control. The control characteristics of the three converters stations are shown in Fig.6, of which, U_{dcref}=10kV, P_{1lref} = -4MW, P_{1href} = 4MW, P_{3ref} = -2MW, U_{dclref} = 9.5kV, U_{dchref} = 10.5kV.

B. *The Results of Simulation*

During the optimization process the system is subjected to 4 steps change of active power in order to experience overvoltage and under voltage operating conditions: at t=1s, the P_{2ref} changed from 7MW to 2MW, at t=2s, it changed from 2MW to -6MW, at t=3s it changed from -6MM to 2MW and at t=4s, it changed from 2MW to 7MW. The PSO algorithm has been implemented in MATLAB environment and its parameters are presented in table I. The table II shows a comparison between SIMPLEX and PSO-optimized parameters, plus their related objective function values.

TABLE I. Parameters of PSO algorithm

Parameter	Particle dimension	Number of particles	Number of iteration	C_1 & C_2	W_{MAX}& W_{MIN}
Value	16	10	60	0.5&0.2	0.9&0.4

TABLE II. Comparison between Simplex and PSO optimized parameters

VSC stations	Controllers loop	SIMPLEX K_1	SIMPLEX T_1	PSO K_1	PSO T_1
VSC_1	U_{dcref}	10	0.0047	15.171	2.2825
	P_{1lref}	0.0010	0.0051	19.348	2.7921
	P_{1href}	0.0010	0.0051	7.1703	0.7135
VSC_2	P_{2ref}	0.002	0.00042	18.549	0.0010
VSC_3	P_{3ref}	0.097	0.00094	15.087	3.0494
	U_{dclref}	5	0.00022	14.010	2.0401
	U_{dchref}	5	0.000049	9.8227	1.5731
$VSC_{1,2,3}$	Q_{ref}	0.01	0.082	15.587	2.374
Objective Function Value		6.06		3.11	

From Table II, it can be seen that the value of ITAE value is about 49% much smaller after optimization with PSO algorithm, which rudely shows the effectiveness of our optimization algorithm. The convergence curve of the objective function value is shown in Fig.7. Fig. 8 illustrates the system dynamic DC voltage and VSC_2 active power responses when subjected to its active power step changes. At t=2s the P_{2ref} changed from 1MW to 5MW, at t=4s it changed from 5MW to -2MW, at t=6s it changed from -6MW to 1MW. As revealed in Figure 8, the optimal coordinated control parameters obtained by the proposed method can control the system more accurately, and can complete the smooth switching of the system when the power changes. The system DC voltage is stable and accurate in steady state, and the control effect is good.

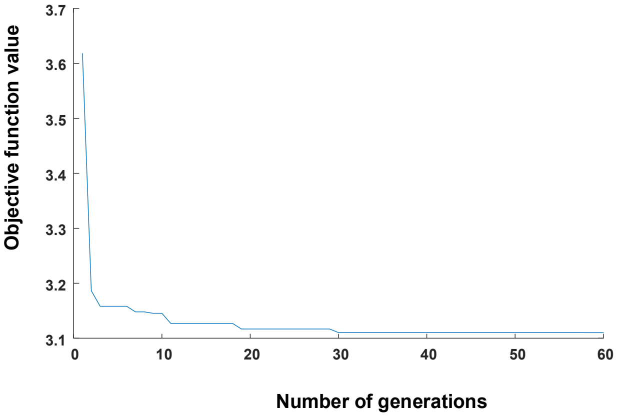

Fig.7. Convergence curve of the objective function value

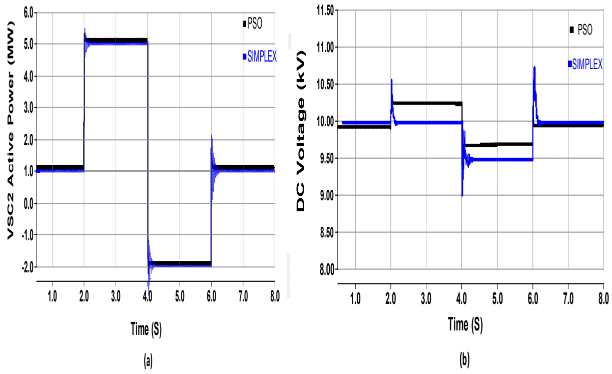

(a)

(b)

Fig.8. System dynamic response when subjected to VSC_2 active power step changes: (a) DC voltage, (b) VSC_2 active power

In order to verify the robustness of our approach, 2 scenarios been studied:

- The main converter VSC_1 is remove from service at t=1s

The system dynamic response while the main converter station is removed from service at t=1s been analyzed and compared. The DC voltage and active powers are shown in Fig.9.

When t=1s, VSC_1 is out of service, the DC system is lacking active power and the DC system voltage drops.

When the voltage drops close to the lower limit U_{dclref} = 9.5kV, VSC_3 is switched from the original active power control to the constant voltage control, the DC voltage is quickly stabilized at 9.5kV, quicker and smoother than using SIMPLEX optimized parameters.

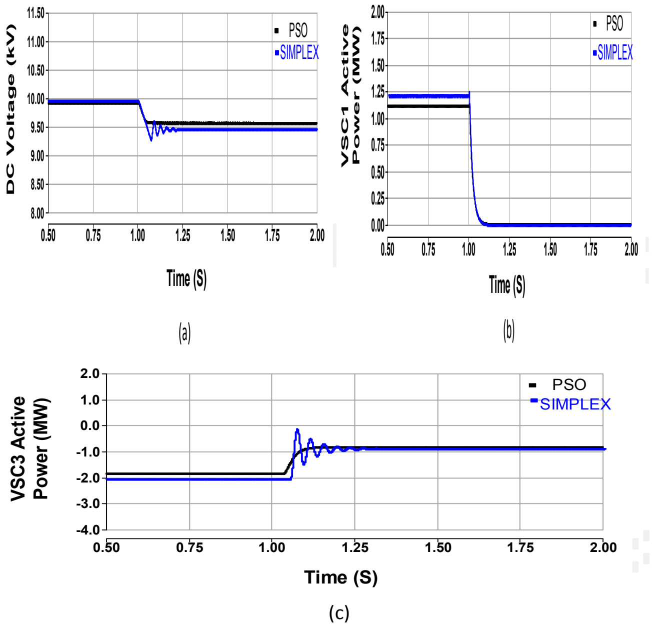

(a)

(b)

(c)

Fig.9. System dynamic response after VSC_1 is out of service: (a) DC voltage, (b) VSC_1 active power, (c) VSC_3 active power
Fig.11. VSC_3 Active power

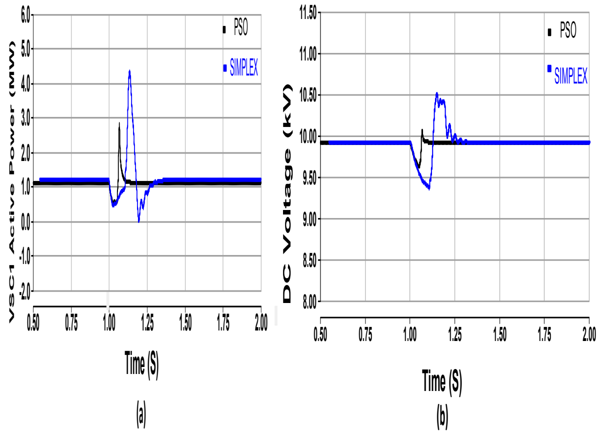

(a)

(b)

Fig.10. System dynamic response DC voltage after three-phase short circuit is applied: (a) VSC_1 active power, (b) DC voltage

VSC$_3$ Active power is also quickly adjusted to balance the system power shortage. The transition process to a new stable state is fast and smooth.

- A three phase short-circuit, located VSC1 AC-side is applied at t=1s,and cleared at t=1.1s

The system dynamic response while a three phase short-circuit, located VSC1 AC-side is applied at t=1s,and cleared at t=1.1s, been analyzed and compared. The DC voltage and active powers are shown in Fig.10.

From figure 10, our approach displays a faster settling time and a lower overvoltage value for dc voltage and active power response. The new optimal PI parameters influence the control dynamic of the VSC converters, such that the system response regain a steady state faster than when it is PI SIMPLEX-optimized. Lower DC voltage and active power peak values are also noticed, which will avoid the deterioration of electric components in the system. The table III shows the different control strategies performance comparison when there is a three phase short-circuit, located VSC1 AC-side. The superiority of the proposed approach is depicted through lower undershoot, overshoot value, and faster settling time.

TABLE III. Performance Comparison

Variables	Undershoot		Overshoot		Settling time	
	PSO	Simplex	PSO	Simplex	PSO	Simplex
Dc Voltage	0.04	0.05	0.008	0.05	1.15	1.26
VSC$_1$ Active power	0.5	0.9	1.47	2.5	1.19	1.35

V. CONCLUSION

In this paper, the simultaneously issues of fast convergence to the global optimum and fast-coordinated dc voltage control at VSC-MTDC level been addressed using a hybrid PSO based multi objective function with different time intervals such that the optimal PI parameters of voltage margin controllers provided a minimum DC voltage deviation and better settling time performance. According to the results of simulation, the robustness of this methodology has been tested and validated.

REFERENCES

[1] M. Starke, F. Li, L. M. Tolbert, and B. Ozpineci, "AC vs. DC distribution: Maximum transfer capability," *IEEE Power Energy Soc. 2008 Gen. Meet. Convers. Deliv. Electr. Energy 21st Century, PES*, 2008.

[2] F. Wang, Y. Pei, D. Boroyevich, R. Burgos, and K. Ngo, "Ac vs. dc distribution for off-shore power delivery," in *IECON Proceedings (Industrial Electronics Conference)*, 2008, pp. 2113–2118.

[3] D. J. Hammerstrom, "AC versus DC distribution systems-did we get it right?," *2007 IEEE Power Eng. Soc. Gen. Meet. PES*, pp. 1–5, 2007.

[4] F. Dastgeer and A. Khalam, "Efficiency comparison of DC and AC distribution systems for distributed generation," in *Power Engineering Conference, 2009.*, 2009, pp. 1–5.

[5] N.R. Chaudhuri, B. Chaudhuri, R. Majumder, and A. Yazdani, Multi-terminal direct current grids. New Jersey: John Wiley & Sons, Inc, 2014.

[6] T. Nakajima and S. Irokawa, "A control system for HVDC transmission by voltage sourced\nconverters," in *1999 IEEE Power Engineering Society Summer Meeting. Conference Proceedings (Cat. No.99CH36364)*, 1999, vol. 2, pp. 1113–1119.

[7] L. Livermore, L. Jun, and J. Ekanayake, "MTDC VSC Technology and its applications for wind power," in *Universities Power Engineering Conference (UPEC), 2010 45th International*, 2010, pp. 1–6.

[8] M. Yang, D. Xie, H. Zhu, and Y. Lou, "Architectures and Control for Multi-terminal DC (MTDC) Distribution Network — A Review," in *AC and DC Power Transmission, 11th IET International Conference on. IET*, 2015, pp. 1–7.

[9] P. Bordignan iiu130 and G. Bathurst, "Delivery of the Nan'ao multi-terminal VSC-HVDC system," in *11th IET International Conference on AC and DC Power Transmission*, 2015, pp. 1–6.

[10] V. Mier, P. G. Casielles, J. Coto, and L. Zeni, "Voltage margin control for offshore multi-use platform integration 553," in *In Proceedings of the 2012 International Con- ference on Renewable Energies and Quality (ICREPQ'12*, 2012, p. 2012.

[11] R. Chai, B. Zhang, and J. Dou, "Improved DC voltage margin control method for DC grid based on VSCs," in *2015 IEEE 15th International Conference on Environment and Electrical Engineering, EEEIC 2015 - Conference Proceedings*, 2015, pp. 1683–1687.

[12] C. Dierckxsens, K. Srivastava, M. Reza, S. Cole, J. Beerten, and R. Belmans, "A distributed DC voltage control method for VSC MTDC systems," *Electr. Power Syst. Res.*, vol. 82, no. 1, pp. 54–58, 2012.

[13] F. D. Bianchi and O. Gomis-Bellmunt, "Droop control design for multi-terminal VSC-HVDC grids based on LMI optimization," in *Proceedings of the IEEE Conference on Decision and Control*, 2011, pp. 4823–4828.

[14] J. Liang and N. Jenkins, "Control of multi-terminal VSC-HVDC transmission for offshore wind power Oriol Gomis-Bellmunt," in *Power Electronics and Applications, 2009. EPE '09. 13th European Conference on*, 2009, pp. 1–10.

[15] H. Li, C. Liu, G. Li, and R. Iravani, "An Enhanced DC Voltage Droop-Control for the VSC-HVDC Grid," *IEEE Trans. Power Syst.*, vol. 8950, no. c, pp. 1–1, 2016.

[16] G. P. Xie and M. X. Wang, "Parameter optimization for current controller in HVDC control system," *2010 Int. Conf. Power Syst. Technol. Technol. Innov. Mak. Power Grid Smarter, POWERCON2010*, 2010.

[17] D. Singh, N. Singh, B. Singh, and S. Prakash, "Optimal gain tuning of PI current controller with parameter uncertainty in DC motor drive for speed control," *2013 Students Conf. Eng. Syst. SCES 2013*, 2013.

[18] Z. Jia and C. Zhao, "Parameters optimization of HVDC control system based on simplex algorithm in RTDS," *2010 5th Int. Conf. Crit. Infrastructure, Cris 2010 - Proc.*, pp. 1–7, 2010.

[19] X. Kang, R. Wang, X. Ma, Q. Ruang, and X. Zhang, "Parameters Optimization of DC V oltage Droop Control Based on VSC-MTDC," *Power Energy Eng. Conf. (APPEEC), 2016 IEEE PES Asia-Pacific*, pp. 2475–2479, 2016.

[20] R. T. Pinto, S. Rodrigues, P. Bauer, and J. Pierik, "Operation and control of a multi-terminal DC network," *2013 IEEE ECCE Asia Downunder - 5th IEEE Annu. Int. Energy Convers. Congr. Exhib. IEEE ECCE Asia 2013*, pp. 474–480, 2013.

[21] Y. Zhang and C. Liu, "Parameters optimal design of HVDC PI controller based on APSO algorithm," in *Asia-Pacific Power and Energy Engineering Conference, APPEEC*, 2012, vol. 2, no. 2.

[22] K. Rouzbehi, A. Miranian, A. Luna, and P. Rodriguez, "Optimized control of multi-terminal DC grids using particle swarm optimization," *EPE J. (European Power Electron. Drives Journal)*, vol. 24, no. 2, pp. 38–49, 2014.

[23] G. P. Inverter, A. Arzani, S. Member, P. Arunagirinathan, and S. Member, "Development of Optimal PI Controllers for a Grid-tied Photovoltaic Inverter," *Comput. Intell. 2015 IEEE Symp. Ser.*, pp. 1272–1279, 2015.

[24] N. Nayak, S. Mishra, S. Choudhury, and P. K. Rout, "Optimal design of VSC based HVDC using Particle Swarm Optimization technique," *2012 2nd Int. Conf. Power, Control Embed. Syst.*, pp. 1–5, 2012.

[25] R. T. Pinto *et al.*, "A Novel Distributed Direct-Voltage Control Strategy for Grid Integration of Offshore Wind Energy Systems Through MTDC Network," vol. 60, no. 6, pp. 2429–2441, 2013.